Molecular Vision 2006; 12:405-14 <http://www.molvis.org/molvis/v12/a47/>
Received 15 April 2005 | Accepted 10 April 2006 | Published 20 April 2006

COX-2 protects against thrombosis of the retinal vasculature in a mouse model of proliferative retinopathy

Lorna M. Cryan,[1] Graham P. Pidgeon,[1] Desmond J. Fitzgerald,[2] Colm J. O'Brien[3]

[1]Department of Clinical Pharmacology, Royal College of Surgeons in Ireland, Dublin, Ireland; Departments of [2]Molecular Medicine and [3]Ophthalmology, Conway Institute of Biomolecular and Biomedical Research, University College Dublin, Dublin, Ireland

Purpose: Cyclooxygenases (COX-1 and COX-2) and prostaglandins regulate angiogenesis in several settings, including cancer and ischemia. In the eye, both selective inhibitors of COX-2 and nonselective COX inhibitors are reported to suppress ischemia-related retinal angiogenesis. Such studies however, may be confounded by the nonspecific effects of inhibitors.

Methods: Mice lacking either the COX-1 (COX-1$^{-/-}$) or COX-2 isoform (COX-2$^{-/-}$) were employed in a model of oxygen-induced retinopathy. Vascular responses were examined by histology, isolectin B4 staining of the abluminal endothelium, and retinal fluorescein angiography.

Results: There was an increase in intravitreal endothelial nuclei in hyperoxia-treated mice compared to normoxic controls irrespective of the genotype. Quantitative analysis of fluorescein-perfused and isolectin B4-stained retinal angiograms at postnatal day 18 (P18) revealed similar global levels of neovascular tufts in hyperoxia-treated wild-type, COX-1$^{-/-}$, and COX-2$^{-/-}$ mice. However, hyperoxia-treated COX-2$^{-/-}$ mice had increased areas of retinal nonperfusion (29.2±1.9 compared to 16.3±2.7; n=6; $p<0.001$). COX-1 disruption had no effect (15.6±2.6; n=8). Platelet deposition within retinal vessels was increased in hyperoxia-treated COX-2$^{-/-}$ mice ($p<0.05$).

Conclusions: Genetic disruption of a single COX isoform is not sufficient to prevent oxygen-induced retinopathy. COX-2 protects retinal vessels from thrombosis, limiting the area of retinal nonperfusion in oxygen-induced retinopathy.

Proliferative diabetic retinal disease is a major cause of blindness in the Western world [1]. Microvascular occlusion leads to both hypoxia and ischemia due to nonperfusion of the inner retina [2-4]. The hypoxic retina responds by generating growth factors, including vascular endothelial growth factor (VEGF), culminating in excessive proliferation of new blood vessels within the retina, often extending into the vitreous [5-8].

The conversion of arachidonic acid to prostaglandin H_2 (PGH_2) by the cyclooxygenase (COX) enzymes is the rate-limiting reaction in the synthesis of prostaglandins [9]. The COX enzymes exist as two distinct isoforms, COX-1 and COX-2. COX-1 is largely a constitutive isoform, whereas COX-2 is induced in response to many different stimuli [9], including ischemia. The products of these enzymes, the prostaglandins, influence a wide range of biological processes of relevance to ischemic proliferative retinopathies. These include vascular tone, platelet activity, inflammation, and angiogenesis [10,11].

Inhibitors of COX suppress angiogenesis in in vitro and in vivo models of excess neovascularization [12-15]. Both COX isoforms have been implicated as signals for angiogenic factors (VEGF, integrin engagement) and as inducers of VEGF expression [16,17]. COX-2 has also been reported to drive the angiogenic response in ocular vascular beds. Disruption of the COX-2 gene inhibits inflammation-induced corneal angiogenesis, but not that induced by VEGF [18]. COX-1 is also reported to regulate the response of endothelial cells to angiogenic factors [19]. Both COX isoforms are expressed in mouse, rat, and human retina [20]. Recent studies have shown that selective and nonselective COX-inhibitors attenuate retinal neovascularization in a mouse model of oxygen-induced retinopathy [21-23].

The aim of the present study was to examine the contribution of each COX isozyme to retinal ischemia and neovascularization by using mice with specific disruption of either the COX-1 or COX-2 isoform in a model of proliferative retinopathy. This approach allows the evaluation of the role of each isoform in oxygen-induced retinopathy without the confounding nonspecific effects of pharmacological COX inhibitors [24].

METHODS

Murine model of oxygen-induced retinopathy: C57BL/6J x 129/Ola mice with a targeted disruption of either the COX-1 gene (COX-1$^{-/-}$) or the COX-2 gene (COX-2$^{-/-}$) were generously provided by R. Langenbach (Laboratory of Environmental Carcinogenesis and Mutagenesis, National Institute of Environmental Health Sciences, National Institute of Health, Triangle Park, NC) [25,26]. The mice were employed in an established model of oxygen-induced retinopathy [27]. Wild-type mice used in these experiments were of the same genetic background (C57BL/6J x 129/Ola). Litters of 7-day-old mice

Correspondence to: Colm O'Brien, MD, Institute of Ophthalmology, Mater Misericordiae Hospital, 60 Eccles Street, Dublin 7, Ireland; Phone: 353-1-8386730; FAX: 353-1-8305693; email: cobrien@mater.ie

were placed, along with their nursing mothers, in an oxygen-regulated chamber under hyperoxic conditions (75% O_2±1.5%) to induce vaso-obliteration and central retinal capillary damage. After five days, the postnatal day 12 (P12) mice and their mothers were removed and kept in normoxic conditions for a further five to six days. All age-matched control animals were raised in normoxic conditions. This study was approved by the Royal College of Surgeons in Ireland's Ethics Committee and was performed under a license from the Department of Health and Children.

Genotyping polymerase chain reactions: Mice were screened for the knockout and wild-type form of COX-1 and COX-2 using polymerase chain reaction (PCR) of tail DNA. The sequences used to amplify the COX-1 gene were wild-type 5'-AGG AGA TGG CTG CTG AGT TGG-3' (601 bp product), knockout 5'-GCA GCC TCT GTT CCA CAT ACA C-3' (646 bp product), and reverse 5'-AAT CTG ACT TTC TGA GTT GCC-3'. The sequences used to amplify the COX-2 gene were wild-type 5'-ACA CAC TCT ATC ACT GGC ACC-3' (760 bp product), knockout 5'-ACG CGT CAC CTT AAT ATG CG-3' (905 bp product), and reverse 5'-ATC CCT TCA CTA AAT GCC CTC-3'. Amplification of 200-300 ng of DNA was performed as follows: 94 °C for 4 min, then 40 cycles at 94 °C for 1 min, 55 °C (COX-1) or 56 °C (COX-2) for 1 min, 72 °C for 1 min, and 72 °C for 7 min. PCR products were then visualized on a 1.2% agarose gel.

Prostaglandin production in the retinas of COX knockout mice: Whole retinas were dissected from normoxia-raised neonatal wild-type, COX-$1^{-/-}$ and COX-$2^{-/-}$ mice, and immediately placed in 500 µl of phosphate-buffered saline (PBS) at 37 °C for 45 min. The supernatant was removed and stored at -80 °C prior to enzyme-immunoassay for prostaglandins and thromboxane. Commercially available enzyme-immunoassay (EIA) kits (Assay Designs, Ann Arbor, MI) were then used to measure 6-keto-$PGF_{1\alpha}$, PGE_2, and TXB_2 levels. These kits use a competitive binding technique, where the prostaglandin in the sample competes with a fixed amount of alkaline-phosphatase-labeled prostaglandin for the binding of a polyclonal antibody immobilized to the wells of the 96 well plate provided. The plate was loaded with 100 µl of each standard or sample. Each sample or standard was incubated with alkaline phosphatase conjugated with the prostaglandin of interest and a monoclonal antibody to the prostaglandin for 2 h at room temperature and 500 RPM. Subsequently, the plate was washed repeatedly and p-nitrophenyl phosphate (pNPP substrate) was added to each well and incubated for 45 min. The optical density of each well was read at 405 nm, with wavelength correction between 600-690 nm, using the Wallac 1420 Manager on the Wallac Victor 2 1420 mutilabel counter (Perkin Elmer, Turku, Finland). Prostaglandin concentration was then calculated using the optical density of the samples in relation to a standard curve.

Quantification of intravitreal neovascularization: Mouse eyes were enucleated, fixed in 4% paraformaldehyde for 24 h, and subsequently embedded in paraffin. Sagittal sections of 5 µm, each 30 µm apart, were cut from each eye parallel to the optic nerve, and stained using hematoxylin and eosin (H & E). Any cell nuclei on the vitreal side of the inner limiting membrane were counted in at least 10 sections from each eye by two independent observers blind to each animal's genotype and treatment (LC and GP). The average intravitreal nuclei/section was calculated for each group. There were at least six animals in each group.

Fluorescein angiography: P12 and P18 mice were deeply anesthetized by an intraperitoneal injection (0.01 ml/g body weight) of a combination of Hypnovel (Roche Products Limited, England) and Hypnorm (Janssen Pharmeceutica, Belgium) diluted in distilled water (final concentrations 1.25 mg/ml midazolam, 2.5 mg/ml fentanyl citrate, 0.079 mg/ml fluanisone). They were then perfused through the left ventricle with 200 µl of 50 mg/ml $2x10^6$ kDa fluorescein-dextran (Sigma, St. Louis, MO) in PBS as previously described [27]. The eyes were enucleated, and placed in 4% paraformaldehyde for 24 h. The retinas were dissected, flat-mounted in Dako mounting medium (DakoCytomation, Glostrup, Denmark), and viewed by confocal scanning laser microscopy (CSLM; MicroRadiance; Bio-Rad, Herts, UK) at a magnification of 4x.

Image analysis of fluorescein angiography: Digital images (magnification 4x) of fluorescein-perfused retinal flatmount preparations were randomized and analyzed by two independent observers (LC and GP) blind to the genotype and treatment represented, using the program Angiostat (Department of Ophthalmology, Queens University, Belfast, Northern Ireland) [28]. This involved evaluating each of the 64 areas that comprise the total flatmount preparation image, as normal vasculature, nonperfused tissue, neovascular tissue, or a combination of these three parameters (Figure 1). The percentage area of nonperfused retina, neovascularization, and normal vasculature was calculated for each image. There were at least six animals per group, and the values for both eyes were averaged.

The degree of central retinal perfusion in fluorescein images (magnification 4x) was further analyzed using Image Pro Plus software (Version 4.0; Media Cybernetics UK, Wokingham, Berkshire, UK). This involved the quantification of nonperfused retina within a defined area located with the optic nerve as the center and 21% of the total 4x image. Focusing on this smaller area ensured that artifacts generated during flatmounting were excluded.

Whole mount isolectin B4 staining: In contrast to fluorescein angiography, isolectin B4 staining of the retinal vasculature allows the visualization of the entire retinal vasculature irrespective of the degree of perfusion. The abluminal side of the endothelium in whole retina preparations was stained with isolectin B4 as previously described in the literature [29]. Briefly, eyes were fixed in 4% paraformaldehyde for at least 6 h, and the retinas were dissected and washed with PBS. Retinas were permeabilized overnight at 4 °C with 0.5% Triton X-100 and 1% BSA in PBS, washed twice with PBS, and incubated with 20 µg/ml biotinylated isolectin B4 (Sigma Aldrich, Dublin, Ireland) at 4 °C overnight. After five PBS washes, the retinas were incubated with 20 µg/ml streptavidin Alexa Fluor® 568 conjugate (Molecular Probes

Europe, Leiden, The Netherlands) for 5 h at 4 °C. Retinas were washed briefly in PBS, placed in 4% paraformaldehyde, flatmounted using Dako mounting medium, and viewed by confocal scanning laser microscopy at a magnification of 4x.

The 4x digital images were analyzed by two independent observers (LC and GP) blind to the genotype and treatment, using the program Angiostat in a similar manner to that described for fluorescein-perfused retinas. There were at least six animals per group, and the values for both eyes were averaged.

Fibrinogen and thrombocyte immunohistochemistry: Paraformaldehyde-fixed, paraffin-embedded sections of 5 μm were deparaffinized and rehydrated, and endogenous peroxidase activity was blocked by placing the tissue in 0.3% H_2O_2 in methanol for 30 min. The sections were incubated in 1.5% normal serum (Vector Laboratories, Burlingame, CA) originating from the species in which the secondary antibody was raised, for 30 min at room temperature. This was followed by incubation for 1 h at room temperature with a goat polyclonal antibody against fibrinogen (Abcam Ltd., Cambridge, UK) diluted 1 in 1,600, or a rabbit polyclonal antimouse thrombocyte antibody (WAK Chemie, Steinbach, Germany) diluted 1 in 2,000. The sections were then incubated with a biotinylated secondary antibody (Vector Laboratories) against the species in which the primary antibody was raised, for 30 min at room temperature. Bound antibody was detected by reaction with horseradish peroxidase-conjugated streptavidin for 30 min, followed by addition of the substrate, diaminobenzidine in PBS for 6 min. Controls included incubation with blocking serum in place of the primary antibody.

Quantitative analysis of thrombocyte staining was performed on at least six sections, 30 μm apart, from each eye as the number of retinal vessel lumina that stained in each section, by an observer (LC) blind to the genotype. Results are given as the average number of stained vessels per section.

Statistical analysis: The results were expressed as mean±standard error of the mean (SEM). Statistical analyses were performed using one-way analysis of variance (ANOVA) where there were more than two groups, using GraphPad InStat 3.0. Where the variation across the groups was significantly greater than expected by chance, the Bonferroni multiple comparisons test was used as a post hoc test. An unpaired Student's t-test was applied to compare the means of two groups. An α level of 0.05 was chosen.

RESULTS

Retinal morphology: Histological analysis of retinal morphology revealed no apparent difference in P17/P18 COX-$1^{-/-}$ or COX-$2^{-/-}$ mice raised in room air in comparison with wild-type controls (Figure 2A). The absence of either enzyme did not appear to effect retinal development or the development of the retinal vasculature.

Retinal prostaglandin production in wild-type, COX-$1^{-/-}$ and COX-$2^{-/-}$ mice: Wild-type retinas produced 474.1±120.9 pg/ml 6-keto-$PGF_{1\alpha}$, 630.3±154.5 pg/ml PGE_2, and 185.2±36.0 pg/ml TXB_2. Retinal production of each of the eicosanoids

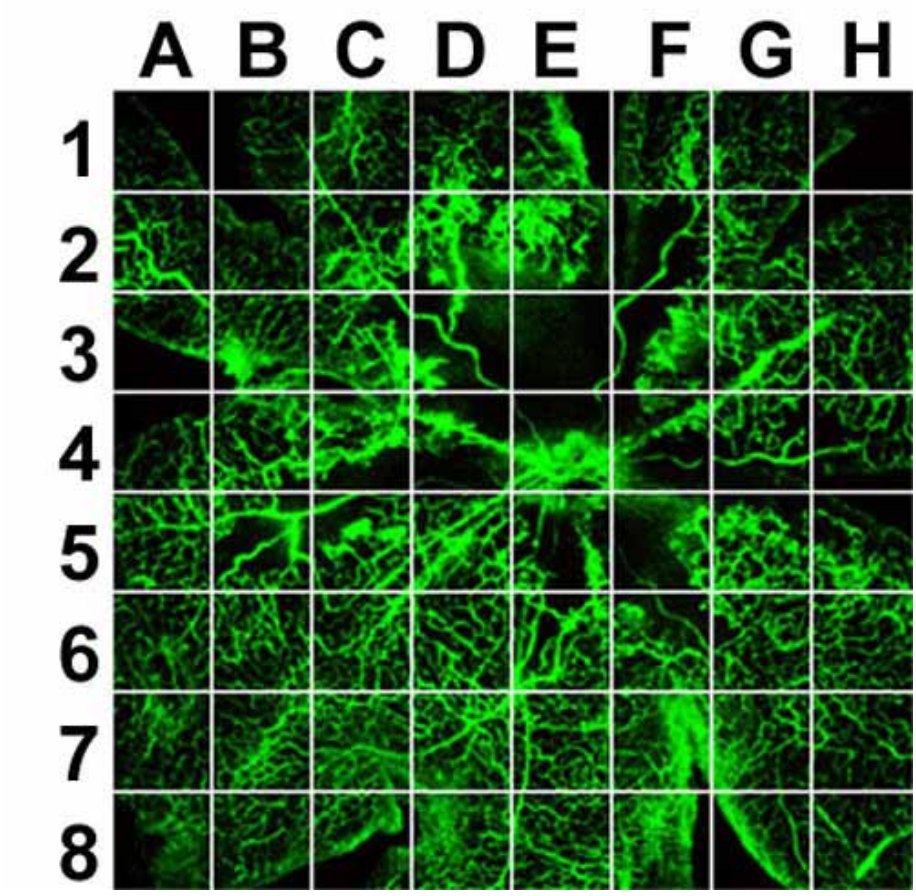

Figure 1. Quantitative analysis of the degree of retinal ischemia and neovascular tuft formation in fluorescein-perfused retinal flatmount preparations. Each of the 64 areas that comprise the total image (magnification 4x) of the retinal flatmount preparation were evaluated by two independent observers as having no retinal tissue present or being empty of tissue (E), normal tissue (N), ischemic/non-perfused tissue (I), or neovascular tuft tissue (T). Up to three annotations were permitted for each area. For example, Area A1 was described as empty (E) and normal (N), area C3 was described as ischemic (I), normal (N) and containing neovascular tufts (T) and area E3 was described as ischemic (I) by both observers. Areas where retinal tissue was absent/empty (E) were subtracted prior to calculation of the percentage area of normal, ischemic or neovascular tissue. Areas where retinal tissue was absent/empty (E) were subtracted prior to calculation of the percentage area of normal, ischemic, or neovascular tissue.

analyzed was significantly decreased in COX-1$^{-/-}$ animals but not in COX-2$^{-/-}$ animals. COX-1$^{-/-}$ retinas produced 12.0±4.9 pg/ml 6-keto-PGF$_{1\alpha}$ (2.5% of wild-type levels $p<0.05$), 59.3±9.1 pg/ml PGE$_2$ (9.4% of wild-type levels, $p<0.05$), and 35.2±3.0 pg/ml TXB$_2$ (19.0% of wild-type levels, $p<0.05$). COX-2$^{-/-}$ retinas produced 508.7±421.1 pg/ml 6-keto-PGF$_{1\alpha}$, 339.2±135.7 pg/ml PGE$_2$ and 86.7±25.2 pg/ml TXB$_2$.

Intravitreal endothelial nuclei in oxygen-induced retinopathy: In this model of proliferative retinopathy, treatment of 7 day-old wild-type mice with hyperoxia (75% oxygen) for five days induces vasoobliteration [8,30]. A return to normoxic conditions for a further five to six days results in uncontrolled proliferation of retinal vessels. New retinal vessels formed neovascular tufts at the vitreal surface of the retina and extended into the vitreous by P18 in wild-type mice (Figure 2A). Counts of intravitreal endothelial cell nuclei were significantly increased ($p<0.001$) in hyperoxia-treated wild-type mice in comparison to room air controls (Figure 2B). Average intravitreal nuclei counts in hyperoxia-treated COX-1$^{-/-}$ and COX-2$^{-/-}$ mice were also significantly increased compared to normoxic controls ($p<0.001$; Figure 2B). There was a nonsignificant ($p>0.05$) trend towards fewer intravitreal nuclei in hyperoxia-treated P18 mice which lacked the COX-2 enzyme as compared to wild-type controls.

Perfused retinal vasculature in oxygen-induced retinopathy: In this model, hyperoxia-treatment of P7 wild-type mice for five days, followed by normoxia for six days, resulted in increased neovascular tuft formation in the whole retina on

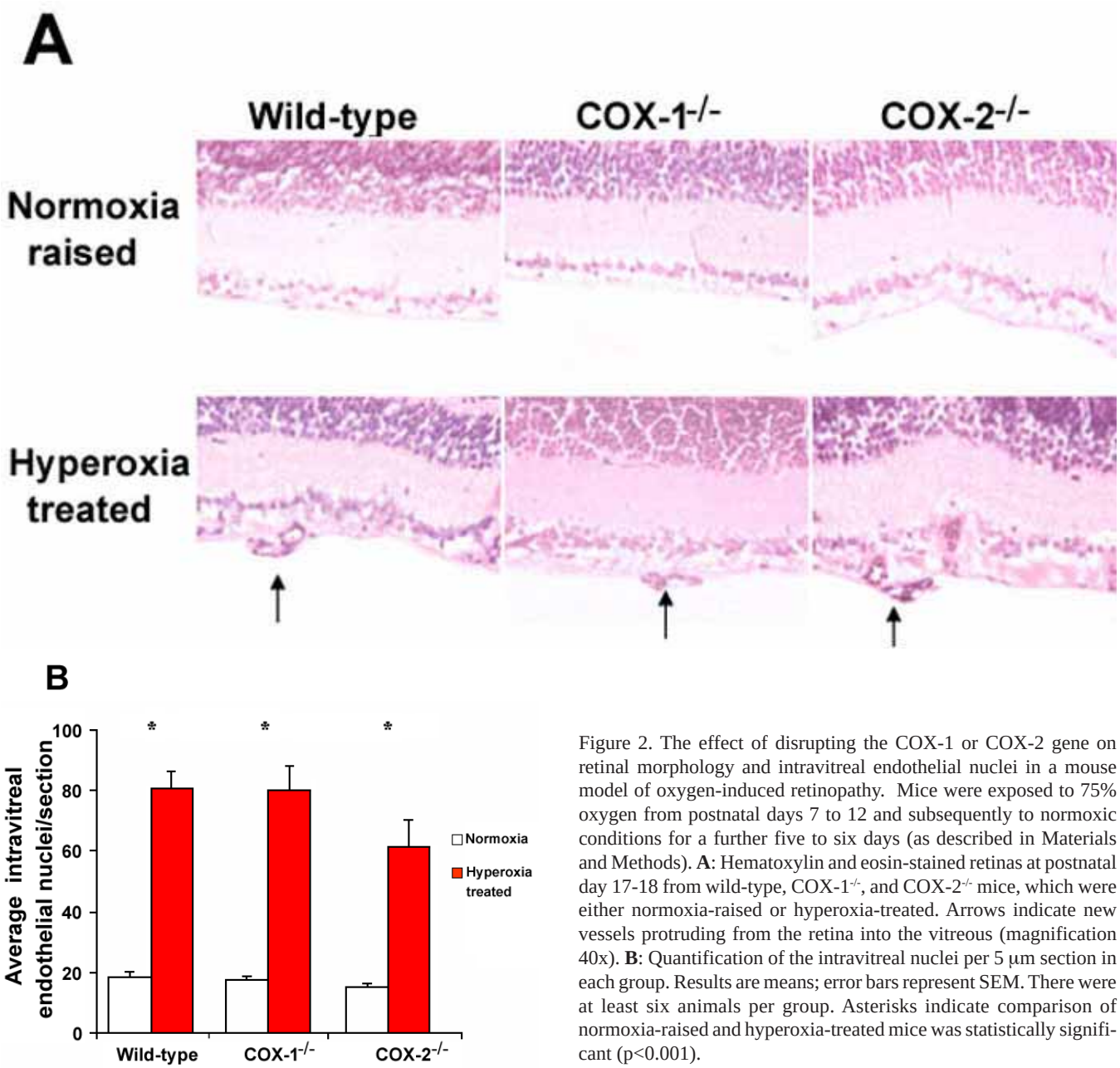

Figure 2. The effect of disrupting the COX-1 or COX-2 gene on retinal morphology and intravitreal endothelial nuclei in a mouse model of oxygen-induced retinopathy. Mice were exposed to 75% oxygen from postnatal days 7 to 12 and subsequently to normoxic conditions for a further five to six days (as described in Materials and Methods). **A**: Hematoxylin and eosin-stained retinas at postnatal day 17-18 from wild-type, COX-1$^{-/-}$, and COX-2$^{-/-}$ mice, which were either normoxia-raised or hyperoxia-treated. Arrows indicate new vessels protruding from the retina into the vitreous (magnification 40x). **B**: Quantification of the intravitreal nuclei per 5 μm section in each group. Results are means; error bars represent SEM. There were at least six animals per group. Asterisks indicate comparison of normoxia-raised and hyperoxia-treated mice was statistically significant ($p<0.001$).

fluorescein angiography at P18 ($p<0.001$; Figure 3A,B). There was no significant difference in neovascular tufts between hyperoxia-treated wild-type, COX-$1^{-/-}$, or COX-$2^{-/-}$ mice, consistent with the counts of intravitreal endothelial nuclei.

There was an increased area of nonperfused retina in wild-type mice ($p<0.001$) following the development of retinopathy (Figure 3C). A similar area of nonperfusion was seen in the COX-$1^{-/-}$ mice. However, hyperoxia-treated COX-$2^{-/-}$ mice had a greater percentage area of retinal nonperfusion when compared with hyperoxia-treated wild-type mice at P18 ($p<0.001$; Figure 3C). This relative increase in nonperfusion of the central retina in COX-$2^{-/-}$ mice ($p<0.001$) was confirmed using Image Pro Plus software (Figure 3D).

We also quantified perfusion in P12 animals. There were no areas of nonperfused retina in normoxia-raised COX-$2^{-/-}$ mice (2.4±1.0) when compared to wild-type mice (1.5±0.7). Following hyperoxia treatment at P12, the percentage area of retinal nonperfusion of COX-$2^{-/-}$ mice (46.5±2.5) was not significantly different to that of wild-type (41.2±2.2) mice. The findings demonstrate that the increase in area of nonperfused retina in COX-$2^{-/-}$ mice at P18 did not arise during hyperoxia but rather occurred as a consequence of events arising during the subsequent normoxia.

Isolectin B4-stained retinal vasculature in oxygen-induced retinopathy: In contrast to the fluorescein angiography, which outlines perfused vessels, isolectin B4 staining identifies the entire retinal vasculature irrespective of perfusion. Analysis of isolectin B4-stained retinas indicated that there was a similar percentage area of capillary-free retina in hyperoxia-treated wild-type (20.6±3.3) and COX-$2^{-/-}$ mice (23.3±3.4) at P18 (Figure 4A,C). Thus, nonperfusion in COX-$2^{-/-}$ animals is not a consequence of a loss of retinal vessels, but is due to vascular obstruction. In accordance with the results from intravitreal endothelial nuclei counts and fluorescein angiography, there was no significant difference in the area of neovascular tuft formation in isolectin-stained retinas between wild-type (22.1±3.1) and COX-$2^{-/-}$ mice (20.2±2.5; Figure 4B).

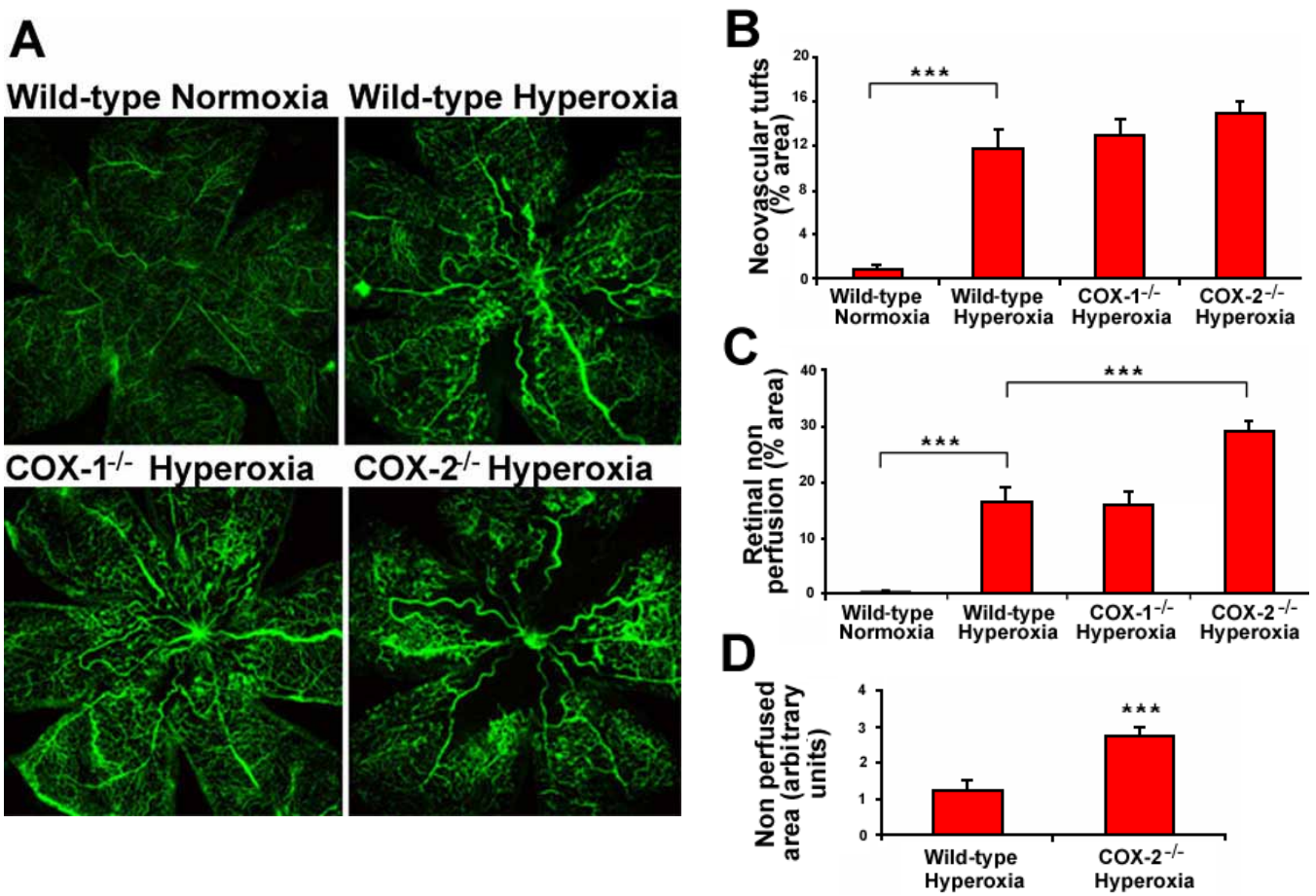

Figure 3. Fluorescein perfused retinal vasculature following oxygen-induced retinopathy in COX knockout mice. Mice were exposed to 75% oxygen from postnatal days 7 to 12 and subsequently to normoxic conditions for a further six days (as described in Materials and Methods). **A**: Deeply anesthetized mice were perfused with fluorescein-dextran, and their retinas flatmounted as described in the Materials and Methods section (magnification 4x). **B**: Quantification of the percentage area of the retina where neovascular tufts were present, in each fluorescein-perfused group at postnatal day 18 (P18) using the program, Angiostat. **C**: Quantification of the percentage area of retinal nonperfusion present in fluorescein-perfused retinal flatmounts at P18 using Angiostat. **D**: Quantification of the area of nonperfused retina, in the central area of interest, in wild-type and COX-$2^{-/-}$ hyperoxia-treated fluorescein-perfused P18 mice using Image Pro Plus. Results are means; error bars represent SEM. There were at least six animals per group. Asterisks indicate comparisons were statistically significant ($p<0.001$).

Retinal fibrinogen and thrombocyte immunolocalization: A polyclonal antibody against fibrinogen was used to detect fibrin [31,32]. Deposition of fibrin was largely absent in normoxia-raised wild-type and COX-2$^{-/-}$ mice and in hyperoxia-treated wild-type mice. In contrast, hyperoxia-treated P18 COX-2$^{-/-}$ mice had deposits of fibrin within many of the smaller inner retinal vessels and those protruding into the vitreous (Figure 5A).

We also detected platelets in retinal vessels using an antibody directed against mouse thrombocytes. Thrombocyte staining was present in the vessels of the inner retina and intravitreal vessels of hyperoxia-treated wild-type and COX-2$^{-/-}$ mice at P18 (Figure 5B). Quantitative assessment of thrombocyte-stained retinal vessels per section demonstrated an increase in the hyperoxia-treated COX-2$^{-/-}$ mice in comparison with wild-type mice ($p<0.05$; Figure 5C). The total number of intraretinal vessels (H & E stained) did not differ between hyperoxia-treated wild-type (34.6±1.5) and COX-2$^{-/-}$ (30.6±2.6) mice, so that the increase in thrombocyte staining in COX-2$^{-/-}$ mice was not due to an increase in the number of vessels.

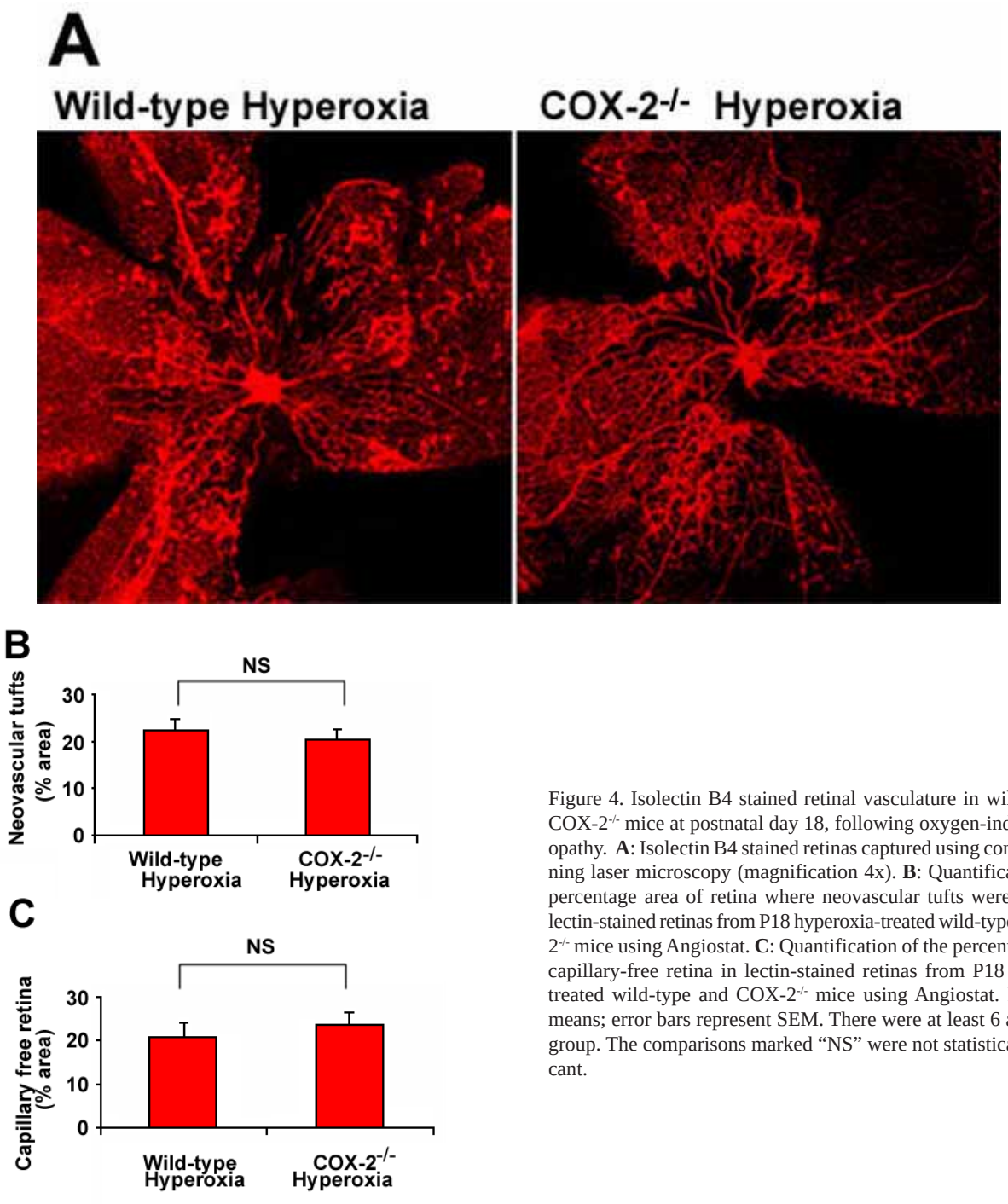

Figure 4. Isolectin B4 stained retinal vasculature in wild-type and COX-2$^{-/-}$ mice at postnatal day 18, following oxygen-induced retinopathy. **A**: Isolectin B4 stained retinas captured using confocal scanning laser microscopy (magnification 4x). **B**: Quantification of the percentage area of retina where neovascular tufts were present in lectin-stained retinas from P18 hyperoxia-treated wild-type and COX-2$^{-/-}$ mice using Angiostat. **C**: Quantification of the percentage area of capillary-free retina in lectin-stained retinas from P18 hyperoxia-treated wild-type and COX-2$^{-/-}$ mice using Angiostat. Results are means; error bars represent SEM. There were at least 6 animals per group. The comparisons marked "NS" were not statistically significant.

DISCUSSION

The selective COX-2 inhibitor, rofecoxib, was reported to increase the risk of myocardial infarction in the Adenomatous Polyp Prevention on Vioxx (APPROVe) study [33,34], resulting in its withdrawal from the market. Concerns have also been raised recently about the cardiovascular safety of a number of other selective COX-2 inhibitors [35,36]. One plausible explanation for this phenomenon is that selective COX-2 inhibition suppresses prostacyclin generated by COX-2 in the vascular endothelium without influencing thromboxane production, as COX-1 within platelets remains active [37]. Prostacyclin inhibits platelet activation, whereas thromboxane is a potent platelet activator. Moreover, platelet-derived thromboxane may act on the vascular endothelium in a paracrine manner to upregulate COX-2 expression and prostacyclin synthesis [38]. The generation of prostacyclin by the vasculature may represent an endogenous mechanism to limit thrombosis when platelets are in contact with the vessel wall.

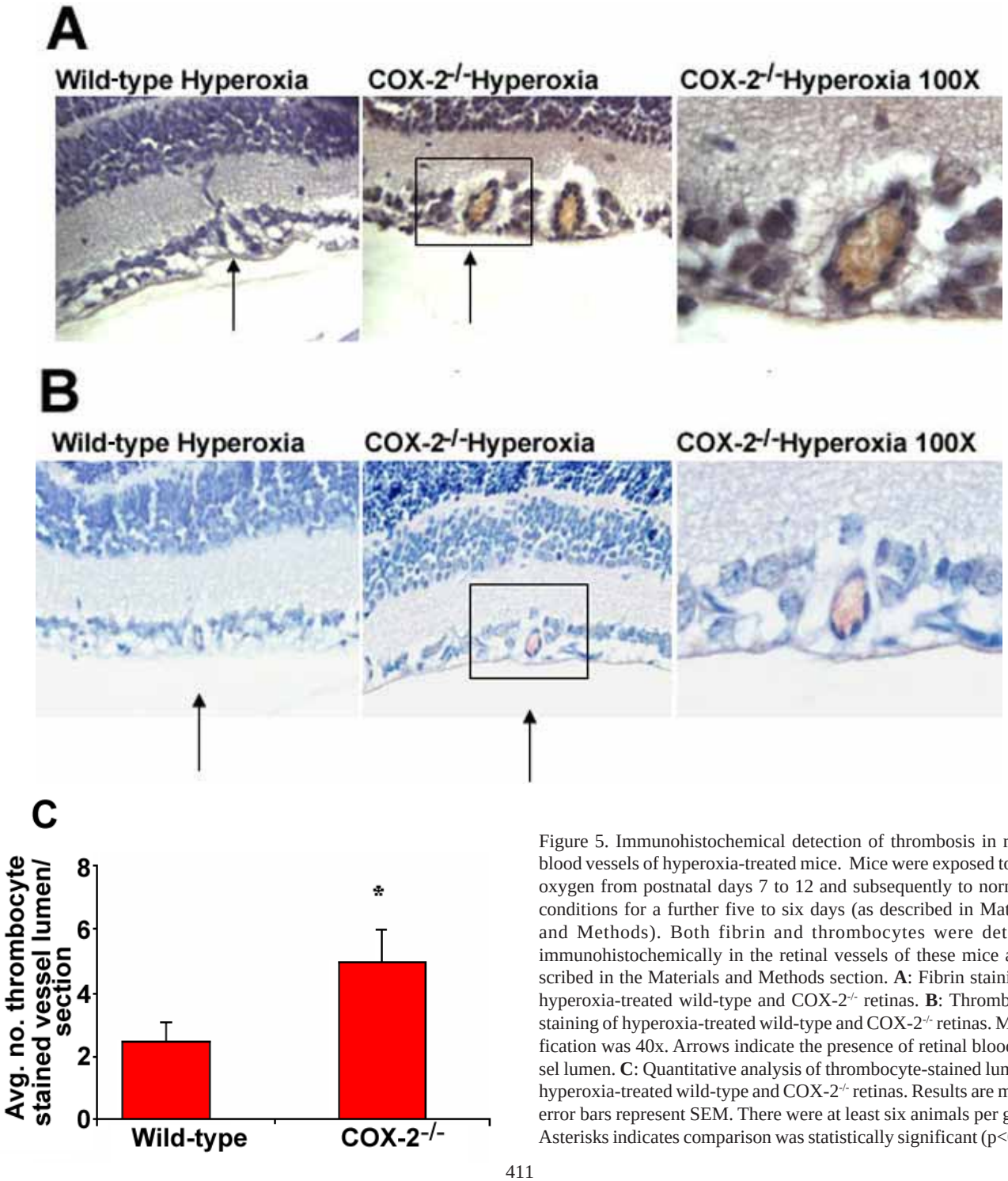

Figure 5. Immunohistochemical detection of thrombosis in retinal blood vessels of hyperoxia-treated mice. Mice were exposed to 75% oxygen from postnatal days 7 to 12 and subsequently to normoxic conditions for a further five to six days (as described in Materials and Methods). Both fibrin and thrombocytes were detected immunohistochemically in the retinal vessels of these mice as described in the Materials and Methods section. **A**: Fibrin staining of hyperoxia-treated wild-type and COX-2$^{-/-}$ retinas. **B**: Thrombocyte staining of hyperoxia-treated wild-type and COX-2$^{-/-}$ retinas. Magnification was 40x. Arrows indicate the presence of retinal blood vessel lumen. **C**: Quantitative analysis of thrombocyte-stained lumen in hyperoxia-treated wild-type and COX-2$^{-/-}$ retinas. Results are means; error bars represent SEM. There were at least six animals per group. Asterisks indicates comparison was statistically significant ($p<0.05$).

The current study identifies a previously undocumented, protective role for COX-2-derived prostaglandins in ischemic retinopathy. The absence of COX-2 increased the area of retinal nonperfusion in a mouse model of oxygen-induced retinopathy. We hypothesize that the retinal nonperfusion is attributable to a shift in the balance between prostacyclin normally generated by COX-2 in the endothelium and thromboxane generated by COX-1 within the platelet. The increase in platelet and fibrin deposits in the retinal vasculature of hyperoxia-treated COX-2$^{-/-}$ mice provides evidence for thrombosis in these animals. A recent study documented retinal vein occlusion in a number of patients following treatment with selective COX-2 inhibitors [39]. Disruption of the COX-2 isoform may also aggravate retinal vasoconstriction, as endothelial prostacyclin has a role in endothelial-dependent relaxation of neonatal retinal blood vessels [40].

We have previously shown that mice deficient in COX-2 exhibit increased deposition of platelets and thrombus formation in comparison with wild-type mice in a model of pulmonary hypertension [41]. In accordance with the current study, we have found that untreated COX-2$^{-/-}$ mice do not have increased platelet deposition in comparison with wild-type mice. The presence of increased thrombosis in COX-2$^{-/-}$ mice in models of vascular injury alone mirrors the situation observed in mice deficient in the receptor for prostacyclin. These mice have normal basal blood pressures, heart rates, and bleeding times, but have they also an increased thrombotic tendency when the endothelium is injured.

In this model of retinopathy, the angiogenic response to hyperoxia-induced vascular damage, occurring during P12 and P18, is two fold. Preretinal neovascular tufts form on the retinal surface and the central retina becomes revascularized. iNOS knockout mice display increased intraretinal revascularization following hyperoxia, and as a consequence of this increased perfusion, have reduced proliferation of preretinal tufts [42].

In our study, we found a similar degree of intraretinal revascularization at P18 in wild-type and COX-2$^{-/-}$ mice, as detected by isolectin B4 staining of the retinal endothelium. The similarity of whole retina endothelial staining between wild-type and COX-2$^{-/-}$ mice also demonstrates that destabilization of newly formed intraretinal vessels in hyperoxia-treated COX-2$^{-/-}$ mice is not contributing to the increased area of nonperfused retina in these mice. Also, our quantitative histological analysis of the number of intraretinal vessels (H & E stained) in hyperoxia-treated wild-type and COX-2$^{-/-}$ mice showed no significant difference between the two groups. These findings, coupled with the discovery of increased thrombocyte deposition in COX-2$^{-/-}$ mice, are consistent with the hypothesis that the protective role of COX-2 in this model of ischemic retinopathy is due to an antithrombotic mechanism rather than the attenuation of intraretinal revascularization.

There were no differences in global neovascular tuft formation in either COX-1$^{-/-}$ or COX-2$^{-/-}$ mice in the model. The findings reported in the present study conflict with those from previous studies where pharmacological inhibition of the COX enzymes was employed. We used three quantitative methods (intravitreal endothelial nuclei, fluorescein perfusion, and isolectin B4 staining) to analyze neovascular tuft formation in these mice. Selective COX-2 inhibitors and nonselective COX-inhibitors have been shown to reduce preretinal neovascularization in models of oxygen-induced retinopathy [21-23]. In addition, Sennlaub et al. [23] reported that inhibition of COX-2 with the preferential COX-2 inhibitors, o-(acetoxyphenyl)hept-2-ynyl sulfide (APHS) and etodolac, from P12-P17 had no effect on the area of nonperfusion in oxygen-induced retinopathy.

Although COX inhibitors are reported to have many effects independent of COX inhibition, these effects generally differ between individual agents [43]. As reduced retinal angiogenesis has now been observed with a number of different structurally unrelated COX inhibitors [21-23], it is unlikely that this is due to COX-independent effects of these compounds, even when considering the results of the present study. On the other hand, studies in knockout animals can be confounded by compensatory changes in the expression of closely related proteins. Our investigation of retinal prostaglandin production in COX knockout mice suggests that compensatory upregulation of the remaining COX isoform does not occur in the retinas of these mice.

Achieving selective inhibition of COX-2 pharmacologically is difficult, and few agents are capable of achieving more than 90% inhibition of COX-2 without concomitant inhibition of COX-1 [44]. The prothrombotic effect of COX-2 inhibition within the retinal endothelium during oxygen-induced retinopathy is not likely to be apparent if COX-1 within the platelet was also inhibited. Conversely, generation of reduced levels of prostacyclin following partial pharmacological inhibition of endothelial COX-2 may still be sufficient to protect retinal vessels from thrombosis. Indeed, animals heterozygote for COX-2, which have been previously shown to express approximately 50% of wild-type COX-2 levels [26], do not exhibit reduced retinal perfusion in this model (data not shown).

In normal circumstances, an increased area of retinal nonperfusion in hyperoxia-treated mice would be expected to lead to a greater retinal angiogenic stimulus and increased neovascularization. However, despite an increased area of retinal nonperfusion, COX-2$^{-/-}$ mice did not display an increase in retinal angiogenesis in comparison with hyperoxia-treated wild-type mice. Although retinal neovascularization was not prevented in COX-2$^{-/-}$ mice, the similar levels of vessel formation, in comparison with wild-type mice, when retinal perfusion was impaired suggests that COX-2 may contribute to retinal angiogenesis to some extent. A direct conclusive evaluation of the contribution of COX-2 to retinal angiogenesis is not possible using mice deficient in COX-2 as a result of our primary finding-increased retinal thrombosis and reduced retinal perfusion in hyperoxia-treated COX-2$^{-/-}$ mice.

In summary, our results demonstrate a protective role for prostaglandins derived from COX-2 activity in ischemic retinopathy. Genetic disruption of a single COX isoform does not prevent oxygen-induced retinopathy. These findings challenge the current concepts of the potential role for COX-2 inhibitors in proliferative retinopathy. Retinal vascular prolif-

eration occurs in a number of diseases, diabetic retinopathy being the most common. Previous in vivo studies have demonstrated that inhibition of COX-2 may protect against nonproliferative features of retinopathy, including leukocyte adhesion to the retinal endothelium and breakdown of the blood retinal barrier [45]. In contrast, our study identifies a potential unfavorable effect of increased retinal thrombosis and occlusion with these agents during proliferative retinopathy. It is likely that COX-2 has a number of different roles in a complex and progressive disease such as diabetic retinopathy. Divergent outcomes may be observed with COX-2 inhibition depending on the stage of the disease and the selectivity of the COX-2 inhibitor.

ACKNOWLEDGEMENTS

The authors would like to acknowledge the assistance and advice of Tom Gardiner and Cliona Boyle at the Department of Ophthalmology, Queens University, Belfast, Northern Ireland. They also thank Robert Langenbach (National Institute of Environmental Health Sciences, Triangle Park, NC) for the gift of COX knockout animals generated in his laboratory.

REFERENCES

1. Aiello LM. Perspectives on diabetic retinopathy. Am J Ophthalmol 2003; 136:122-35.
2. Brown GC, Magargal LE, Federman JL. Ischaemia and neovascularization. Trans Ophthalmol Soc U K 1980; 100:377-80.
3. Boeri D, Maiello M, Lorenzi M. Increased prevalence of microthromboses in retinal capillaries of diabetic individuals. Diabetes 2001; 50:1432-9.
4. Schroder S, Palinski W, Schmid-Schonbein GW. Activated monocytes and granulocytes, capillary nonperfusion, and neovascularization in diabetic retinopathy. Am J Pathol 1991; 139:81-100.
5. Simpson DA, Murphy GM, Bhaduri T, Gardiner TA, Archer DB, Stitt AW. Expression of the VEGF gene family during retinal vaso-obliteration and hypoxia. Biochem Biophys Res Commun 1999; 262:333-40.
6. Pierce EA, Avery RL, Foley ED, Aiello LP, Smith LE. Vascular endothelial growth factor/vascular permeability factor expression in a mouse model of retinal neovascularization. Proc Natl Acad Sci U S A 1995; 92:905-9.
7. Adamis AP, Miller JW, Bernal MT, D'Amico DJ, Folkman J, Yeo TK, Yeo KT. Increased vascular endothelial growth factor levels in the vitreous of eyes with proliferative diabetic retinopathy. Am J Ophthalmol 1994; 118:445-50.
8. Pierce EA, Foley ED, Smith LE. Regulation of vascular endothelial growth factor by oxygen in a model of retinopathy of prematurity. Arch Ophthalmol 1996; 114:1219-28. Erratum in: Arch Ophthalmol 1997; 115:427.
9. Smith WL, Dewitt DL. Prostaglandin endoperoxide H synthases-1 and -2. Adv Immunol 1996; 62:167-215.
10. Iniguez MA, Rodriguez A, Volpert OV, Fresno M, Redondo JM. Cyclooxygenase-2: a therapeutic target in angiogenesis. Trends Mol Med 2003; 9:73-8.
11. Davidge ST. Prostaglandin H synthase and vascular function. Circ Res 2001; 89:650-60.
12. Leahy KM, Ornberg RL, Wang Y, Zweifel BS, Koki AT, Masferrer JL. Cyclooxygenase-2 inhibition by celecoxib reduces proliferation and induces apoptosis in angiogenic endothelial cells in vivo. Cancer Res 2002; 62:625-31.
13. Kawamori T, Rao CV, Seibert K, Reddy BS. Chemopreventive activity of celecoxib, a specific cyclooxygenase-2 inhibitor, against colon carcinogenesis. Cancer Res 1998; 58:409-12.
14. Yamada M, Kawai M, Kawai Y, Mashima Y. The effect of selective cyclooxygenase-2 inhibitor on corneal angiogenesis in the rat. Curr Eye Res 1999; 19:300-4.
15. Daniel TO, Liu H, Morrow JD, Crews BC, Marnett LJ. Thromboxane A2 is a mediator of cyclooxygenase-2-dependent endothelial migration and angiogenesis. Cancer Res 1999; 59:4574-7.
16. Murphy JF, Fitzgerald DJ. Vascular endothelial growth factor induces cyclooxygenase-dependent proliferation of endothelial cells via the VEGF-2 receptor. FASEB J 2001; 15:1667-9.
17. Williams CS, Tsujii M, Reese J, Dey SK, DuBois RN. Host cyclooxygenase-2 modulates carcinoma growth. J Clin Invest 2000; 105:1589-94.
18. Kuwano T, Nakao S, Yamamoto H, Tsuneyoshi M, Yamamoto T, Kuwano M, Ono M. Cyclooxygenase 2 is a key enzyme for inflammatory cytokine-induced angiogenesis. FASEB J 2004; 18:300-10.
19. Tsujii M, Kawano S, Tsuji S, Sawaoka H, Hori M, DuBois RN. Cyclooxygenase regulates angiogenesis induced by colon cancer cells. Cell 1998; 93:705-16. Erratum in: Cell 1998; 94:following 271.
20. Ju WK, Neufeld AH. Cellular localization of cyclooxygenase-1 and cyclooxygenase-2 in the normal mouse, rat, and human retina. J Comp Neurol 2002; 452:392-9.
21. Takahashi K, Saishin Y, Saishin Y, Mori K, Ando A, Yamamoto S, Oshima Y, Nambu H, Melia MB, Bingaman DP, Campochiaro PA. Topical nepafenac inhibits ocular neovascularization. Invest Ophthalmol Vis Sci 2003; 44:409-15.
22. Wilkinson-Berka JL, Alousis NS, Kelly DJ, Gilbert RE. COX-2 inhibition and retinal angiogenesis in a mouse model of retinopathy of prematurity. Invest Ophthalmol Vis Sci 2003; 44:974-9.
23. Sennlaub F, Valamanesh F, Vazquez-Tello A, El-Asrar AM, Checchin D, Brault S, Gobeil F, Beauchamp MH, Mwaikambo B, Courtois Y, Geboes K, Varma DR, Lachapelle P, Ong H, Behar-Cohen F, Chemtob S. Cyclooxygenase-2 in human and experimental ischemic proliferative retinopathy. Circulation 2003; 108:198-204.
24. Samaha HS, Kelloff GJ, Steele V, Rao CV, Reddy BS. Modulation of apoptosis by sulindac, curcumin, phenylethyl-3-methylcaffeate, and 6-phenylhexyl isothiocyanate: apoptotic index as a biomarker in colon cancer chemoprevention and promotion. Cancer Res 1997; 57:1301-5.
25. Langenbach R, Morham SG, Tiano HF, Loftin CD, Ghanayem BI, Chulada PC, Mahler JF, Lee CA, Goulding EH, Kluckman KD, Kim HS, Smithies O. Prostaglandin synthase 1 gene disruption in mice reduces arachidonic acid-induced inflammation and indomethacin-induced gastric ulceration. Cell 1995; 83:483-92.
26. Morham SG, Langenbach R, Loftin CD, Tiano HF, Vouloumanos N, Jennette JC, Mahler JF, Kluckman KD, Ledford A, Lee CA, Smithies O. Prostaglandin synthase 2 gene disruption causes severe renal pathology in the mouse. Cell 1995; 83:473-82.
27. Smith LE, Wesolowski E, McLellan A, Kostyk SK, D'Amato R, Sullivan R, D'Amore PA. Oxygen-induced retinopathy in the mouse. Invest Ophthalmol Vis Sci 1994; 35:101-11.
28. Gebarowska D, Stitt AW, Gardiner TA, Harriott P, Greer B, Nelson J. Synthetic peptides interacting with the 67-kd laminin recep-

tor can reduce retinal ischemia and inhibit hypoxia-induced retinal neovascularization. Am J Pathol 2002; 160:307-13.
29. Gerhardt H, Golding M, Fruttiger M, Ruhrberg C, Lundkvist A, Abramsson A, Jeltsch M, Mitchell C, Alitalo K, Shima D, Betsholtz C. VEGF guides angiogenic sprouting utilizing endothelial tip cell filopodia. J Cell Biol 2003; 161:1163-77.
30. Ishida S, Yamashiro K, Usui T, Kaji Y, Ogura Y, Hida T, Honda Y, Oguchi Y, Adamis AP. Leukocytes mediate retinal vascular remodeling during development and vaso-obliteration in disease. Nat Med 2003; 9:781-8.
31. Smyth SS, Reis ED, Vaananen H, Zhang W, Coller BS. Variable protection of beta 3-integrin—deficient mice from thrombosis initiated by different mechanisms. Blood 2001; 98:1055-62.
32. Yanada M, Kojima T, Ishiguro K, Nakayama Y, Yamamoto K, Matsushita T, Kadomatsu K, Nishimura M, Muramatsu T, Saito H. Impact of antithrombin deficiency in thrombogenesis: lipopolysaccharide and stress-induced thrombus formation in heterozygous antithrombin-deficient mice. Blood 2002; 99:2455-8.
33. Bresalier RS, Sandler RS, Quan H, Bolognese JA, Oxenius B, Horgan K, Lines C, Riddell R, Morton D, Lanas A, Konstam MA, Baron JA, Adenomatous Polyp Prevention on Vioxx (APPROVe) Trial Investigators. Cardiovascular events associated with rofecoxib in a colorectal adenoma chemoprevention trial. N Engl J Med 2005; 352:1092-102.
34. Fitzgerald GA. Coxibs and cardiovascular disease. N Engl J Med 2004; 351:1709-11.
35. Nussmeier NA, Whelton AA, Brown MT, Langford RM, Hoeft A, Parlow JL, Boyce SW, Verburg KM. Complications of the COX-2 inhibitors parecoxib and valdecoxib after cardiac surgery. N Engl J Med 2005; 352:1081-91.
36. Solomon SD, McMurray JJ, Pfeffer MA, Wittes J, Fowler R, Finn P, Anderson WF, Zauber A, Hawk E, Bertagnolli M, Adenoma Prevention with Celecoxib (APC) Study Investigators. Cardiovascular risk associated with celecoxib in a clinical trial for colorectal adenoma prevention. N Engl J Med 2005; 352:1071-80.
37. Belton O, Byrne D, Kearney D, Leahy A, Fitzgerald DJ. Cyclooxygenase-1 and -2-dependent prostacyclin formation in patients with atherosclerosis. Circulation 2000; 102:840-5.
38. Caughey GE, Cleland LG, Gamble JR, James MJ. Up-regulation of endothelial cyclooxygenase-2 and prostanoid synthesis by platelets. Role of thromboxane A2. J Biol Chem 2001; 276:37839-45.
39. Meyer CH, Schmidt JC, Rodrigues EB, Mennel S. Risk of retinal vein occlusions in patients treated with rofecoxib (vioxx). Ophthalmologica 2005; 219:243-7.
40. Hardy P, Abran D, Hou X, Lahaie I, Peri KG, Asselin P, Varma DR, Chemtob S. A major role for prostacyclin in nitric oxide-induced ocular vasorelaxation in the piglet. Circ Res 1998; 83:721-9.
41. Pidgeon GP, Tamosiuniene R, Chen G, Leonard I, Belton O, Bradford A, Fitzgerald DJ. Intravascular thrombosis after hypoxia-induced pulmonary hypertension: regulation by cyclooxygenase-2. Circulation 2004; 110:2701-7.
42. Sennlaub F, Courtois Y, Goureau O. Inducible nitric oxide synthase mediates the change from retinal to vitreal neovascularization in ischemic retinopathy. J Clin Invest 2001; 107:717-25.
43. Baek SJ, Wilson LC, Lee CH, Eling TE. Dual function of nonsteroidal anti-inflammatory drugs (NSAIDs): inhibition of cyclooxygenase and induction of NSAID-activated gene. J Pharmacol Exp Ther 2002; 301:1126-31.
44. Warner TD, Giuliano F, Vojnovic I, Bukasa A, Mitchell JA, Vane JR. Nonsteroid drug selectivities for cyclo-oxygenase-1 rather than cyclo-oxygenase-2 are associated with human gastrointestinal toxicity: a full in vitro analysis. Proc Natl Acad Sci U S A 1999; 96:7563-8. Erratum in: Proc Natl Acad Sci U S A 1999; 96:9666.
45. Joussen AM, Poulaki V, Mitsiades N, Kirchhof B, Koizumi K, Dohmen S, Adamis AP. Nonsteroidal anti-inflammatory drugs prevent early diabetic retinopathy via TNF-alpha suppression. FASEB J 2002; 16:438-40.

The print version of this article was created on 20 Apr 2006. This reflects all typographical corrections and errata to the article through that date. Details of any changes may be found in the online version of the article.